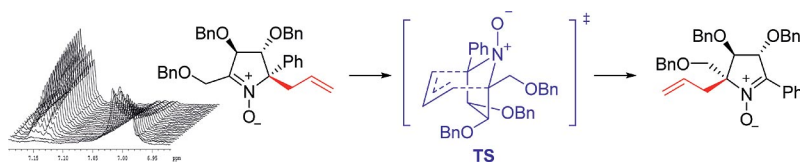


Aza-Cope Rearrangement

The hitherto unknown neutral 2-aza-Cope rearrangement of nitrones takes place under thermal conditions with complete transfer of chirality. The process can be catalyzed by acid through a classical cationic

2-aza-Cope rearrangement. Kinetic ^1H NMR experiments and DFT theoretical studies have been used to estimate the activation parameters and determine the energy of activation of the process.

**I. Delso, A. Melicchio, A. Isasi, T. Tejero,
P. Merino*** 1–11

Evasive Neutral 2-Aza-Cope Rearrangements. Kinetic and Computational Studies with Cyclic Nitrones 

Keywords: Aza-Cope rearrangement / Kinetics / Nitrones / Density functional calculations / Allylation

DOI: 10.1002/ejoc.201300836

Evasive Neutral 2-Aza-Cope Rearrangements. Kinetic and Computational Studies with Cyclic Nitrones

Ignacio Delso,^[a,b] Alessandro Melicchio,^{[a],[*]} Arantzazu Isasi,^[a] Tomás Tejero,^[a] and Pedro Merino^{*[a]}

Dedicated to Professor Giovanni Romeo on the occasion of his 70th birthday

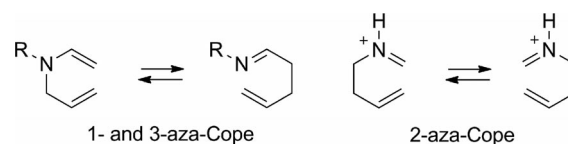
Keywords: Aza-Cope rearrangement / Kinetics / Nitrones / Density functional calculations / Allylation

A full experimental study of the activation energy required for the hitherto unknown neutral 2-aza-Cope rearrangement is presented. A kinetic study of the process showed activation energies in the range of 22.91–24.06 kcal/mol, in agreement with a process operating at moderate temperature (70 °C). Calculations at B3LYP/6-311+G(d,p) and M06-2X/6-311+G(d,p) levels of theory considering solvent (dimethyl sulfoxide (DMSO) and toluene) effects (PCM model) predict reaction energy barriers that are in agreement with the values obtained from ¹H NMR-based kinetic experiments. Re-

sults obtained by using enantiomerically pure substrates demonstrate that the rearrangement takes place with complete transfer of chirality, in contrast to previously described cationic processes. The effects of solvent and acid catalysis, which converts the process into the more common cationic rearrangement, have also been studied. DFT calculations also predict correctly the acceleration of the process under acid catalysis, estimating energy barriers in the range of 16.80–18.57 kcal/mol.

Introduction

Stereoselective [3,3]-sigmatropic processes are well-known and powerful tools in organic synthesis.^[1] Among them, Claisen^[2] and Cope^[3] rearrangements have developed exceptionally well in the past 50 years. In particular, aza-Cope rearrangements have attracted great interest because of the ubiquitous presence of nitrogen-containing structures in natural and biological products as well as synthetic intermediates. Moreover, the merging of aza-Cope rearrangements with other reactions such as [3+2] cycloaddition^[4] or Mannich type reaction^[5] provide direct access to a variety of complex structures. Depending on the position of the nitrogen atom, several aza-Cope rearrangements can be identified (Scheme 1).



Scheme 1. Aza-Cope rearrangements.

The 1-aza-Cope rearrangement, developed by Fowler and co-workers from aza-diene precursors,^[6] has been used in the synthesis of nitrogen heterocycles.^[7] In 1992, Stille and co-workers reported the inverse process as a 3-aza-Cope rearrangement starting from *N*-alkyl-*N*-allylenamines.^[8] This reaction has also been studied for quaternary *N*-allyl enammonium salts.^[9]

Both 1- and 3-aza-Cope rearrangements are thermal processes that are catalyzed by Lewis acids. The 2-aza-Cope rearrangement had only been described as an equilibrium system for cationic substrates,^[10] and several protocols were developed to drive the process to a single product.^[11] These protocols included trapping the iminium ion with a nucleophile incorporated into the structure^[12] and a Mannich type reaction.^[13] The synthetic utility of the reaction has been extensively demonstrated^[14] and, more recently, a catalytic asymmetric version has been reported for protonated imines.^[15]

Wuts and Jung reported the 2-aza-Cope rearrangement of nitrones under catalysis with trimethylsilyl triflate,^[16]

[a] Laboratorio de Síntesis Asimétrica, Departamento de Síntesis y Estructura de Biomoléculas, Instituto de Síntesis Química y Catálisis Homogénea (ISQCH), Universidad de Zaragoza, CSIC, 50009 Zaragoza, Aragón, Spain
E-mail: pmerino@unizar.es
Homepage: <http://www.bioorganica.es>

[b] Servicio de Resonancia Magnética Nuclear, Centro de Química y Materiales de Aragón (CEQMA), Universidad de Zaragoza, CSIC, 50009 Zaragoza, Aragón, Spain

[*] Present address: Dipartimento di Chimica e Tecnologie Chimiche, Università della Calabria, via Bucci 12 C, 87036 Rende (CS), Italy

Supporting information for this article is available on the WWW under <http://dx.doi.org/10.1002/ejoc.201300836>.

which actually involves hydroxyiminium cations. A similar process was described twenty years later by Loh and co-workers using 10-camphorsulfonic acid (CSA) as a catalyst.^[17] In both cases, the rearrangement involved cationic species, as in other 2-aza-Cope rearrangements. On the other hand, the possibility of inducing a thermal 2-aza-Cope rearrangement with neutral substrates had only been suggested,^[18] and in 2007 we reported for the first time experimental and theoretical evidence of a neutral thermal 2-aza-Cope rearrangement of nitrones.^[19] As far as we are aware there are no examples in the literature concerning thermal 2-aza-Cope rearrangements with neutral substrates other than those reported from our laboratory.^[20]

In this paper, we report a full experimental study based on NMR kinetic experiments of the activation energies required for both neutral and catalyzed 2-aza-Cope rearrangements of nitrones. DFT calculations are also used to compare experimental and theoretical values for noncatalyzed vs. catalyzed processes. The study has been extended to include cyclic nitrones **1** and **2** and, ultimately, applied to the rearrangement of enantiomerically pure nitrone **3** (Figure 1).

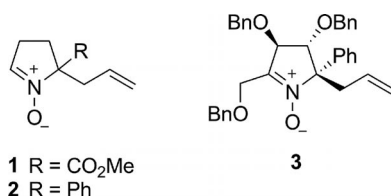


Figure 1. Cyclic nitrones.

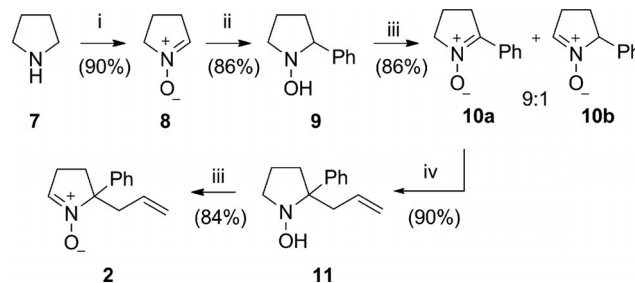
Results and Discussion

Preparation of Nitrones

Nitrone **1** was prepared starting from methyl prolinolate **4** (Scheme 2). Oxidation of **4** catalyzed by methyltrioxorhenium^[21] afforded nitrone **5** in 80% yield.^[22] Compound **5** was also reported to be obtained from **4** by oxidation with hydrogen peroxide in the presence of a catalytic amount of sodium tungstate, but only in 42% yield.^[23] Further allylation^[24] of **5** to give **6** and subsequent oxidation with manganese(IV) oxide^[25] provided nitrone **1** in 58% overall yield (three steps) from **4**.

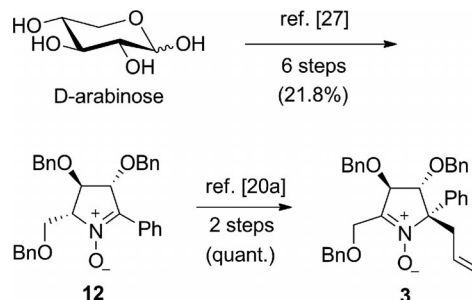
Nitrone **2** was prepared from nitrone **8**, which was obtained by oxidation of pyrrolidine **7** with methyltrioxorhenium as described (Scheme 3).^[26] After nucleophilic addition of phenylmagnesium bromide and oxidation with manganese(IV) oxide,^[25] a 9:1 mixture of nitrones **10a** and **10b**

was obtained. The major isomer **10a** was separated by chromatography and allylated following our standard procedure^[24] to give hydroxylamine **11**. Finally, oxidation of **11** furnished nitrone **2** in 48% overall yield (five steps).



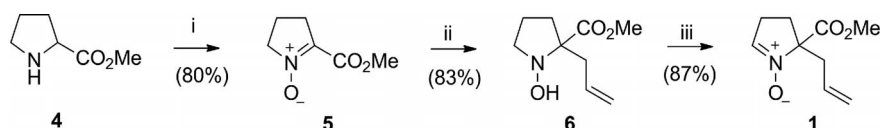
Scheme 3. Synthesis of nitrone **2**. *Reagents and conditions:* (i) MeReO₃ (2 mol-%), UHP, MeOH, room temp., 24 h; (ii) phenylmagnesium bromide, THF 0 °C, 2 h; (iii) MnO₂, CH₂Cl₂, 0 °C, 7 h; (iv) allylmagnesium bromide, THF 0 °C, 8 h.

Nitrone **3** was prepared with complete selectivity and quantitative yield from nitrone **12**,^[20a] which was obtained from D-arabinose in six steps and 21.8% overall yield (Scheme 4).^[27]

Scheme 4. Synthesis of nitrone **3**.

Kinetic Studies

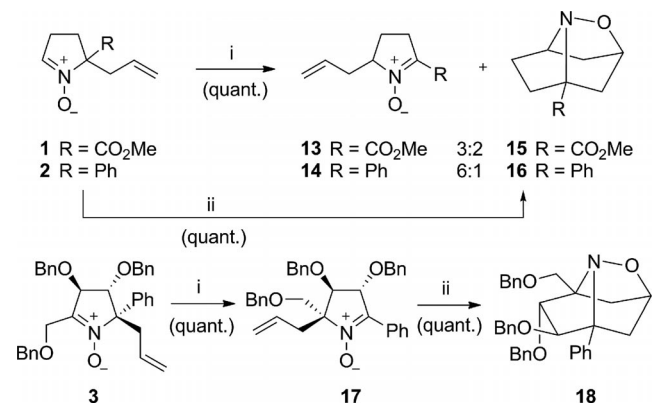
Heating nitrones **1** or **2** in dimethyl sulfoxide (DMSO) in a sealed tube at 70 °C for 6 h afforded mixtures of rearranged nitrones and the corresponding cycloadducts formed through an intramolecular 1,3-dipolar cycloaddition (Scheme 5). Prolonged heating for 36 h only provided cycloadducts **15** and **16**, in quantitative yield, from nitrones **1** and **2**, respectively, indicating that nitrones **13** and **14** are intermediates of the reaction. On the other hand, nitrone **17** was obtained from nitrone **3** in quantitative yield and complete selectivity under the same reaction conditions.



Scheme 2. Synthesis of nitrone **1**. *Reagents and conditions:* (i) MeReO₃ (2 mol-%), urea–hydrogen peroxide (UHP) complex, MeOH, room temp., 24 h; (ii) allylmagnesium bromide, THF 0 °C, 8 h; (iii) MnO₂, CH₂Cl₂, 0 °C, 7 h.

FULL PAPER

Prolonged heating of isolated **17** (or directly from **3**) ultimately led to the corresponding cycloadduct **18**, as described.^[20a]



Scheme 5. Rearrangement of nitrones **1–3**. Reagents and conditions: (i) DMSO, 70 °C, 6 h, sealed tube; (ii) toluene 120 °C, 36 h, sealed tube.

To obtain detailed information on the factors and activation energy of the process, we investigated the rearrangement of nitrones **1–3** by ¹H NMR spectroscopic analysis at a range of temperatures between 40–90 °C, and determined the activation parameters. The disappearance of the NMR signal of nitrone **3** at $\delta = 7.00$ ppm with the appearance of the NMR signal of nitrone **17** at $\delta = 7.14$ ppm, as shown in Figure 2, is evidence that the process monitored is that illustrated in Scheme 5. Similar kinetic NMR runs were performed for nitrones **1** and **2**. The changes in concentration of nitrones **1–3** were determined from the corresponding ¹H NMR spectra by measuring integral data. In the case of nitrones **1** and **2**, we ascertained that the relationship between the concentration of the rearranged nitrones **13** and **14** and the corresponding starting nitrones is best described by a straight line, which is a mathematical proof

that the thermal 2-aza-Cope rearrangement takes place prior to the cycloaddition reaction. Indeed, a plot of the natural logarithm of concentration, i.e., $\ln(\chi)$, against time, was a straight line, confirming that the process is first-order in all cases. From the reaction conducted at various temperatures (40–90 °C), the corresponding kinetic constants were calculated for each temperature. The Arrhenius plot (see the Supporting Information) permitted evaluation of the respective activation energies and Eyring plots (Figure 3), a direct evaluation of the activation parameters ΔH^\ddagger and ΔS^\ddagger and, in consequence ΔG^\ddagger at 298.15 K (Table 1). In all cases, all the values were similar and activation energies were found to be within a range of 1.2 kcal/mol (from 22.91 to 23.16 kcal/mol).

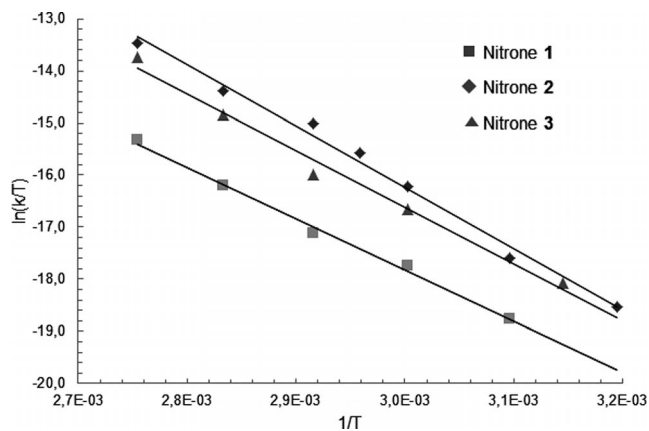


Figure 3. Eyring plots [$\ln(K/T)$ vs. $1/T$] for rearrangements of nitrones **1–3**.

We also investigated the rearrangement of nitrone **2** in toluene and under acid catalysis. Thus, the same reactivity illustrated in Scheme 5 was observed in toluene, although the reaction was completed in 4 h, in agreement with a neutral pericyclic transition state,^[19] which should be stabilized

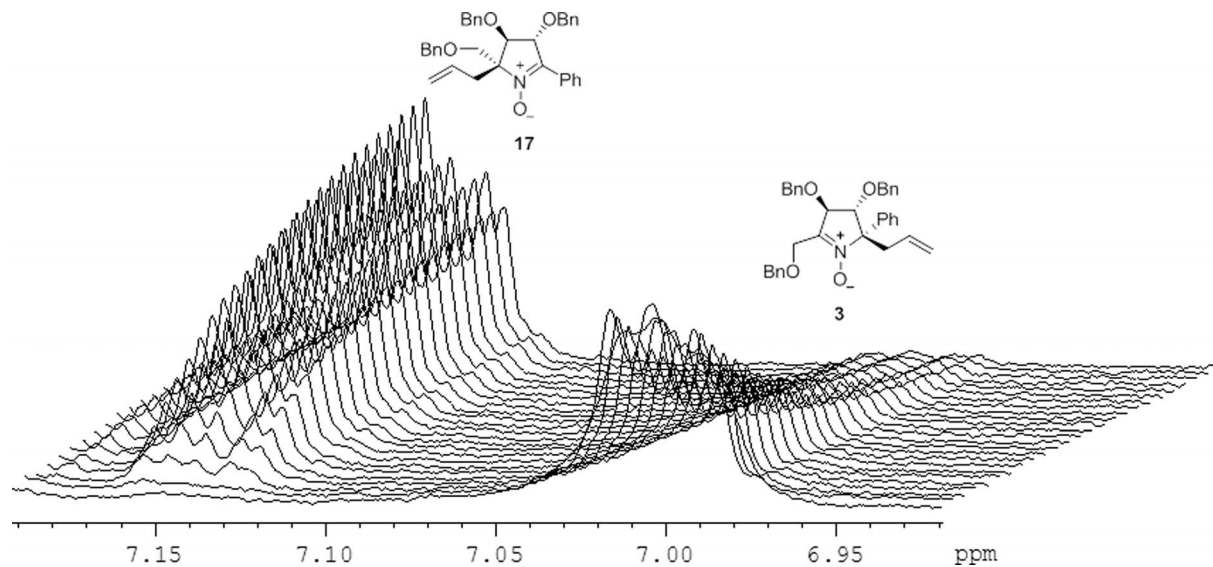


Figure 2. Stack plot illustrating ¹H NMR signals (aromatic protons) for starting nitrone **3** and rearranged nitrone **17** at 343 K, at 30 min intervals.

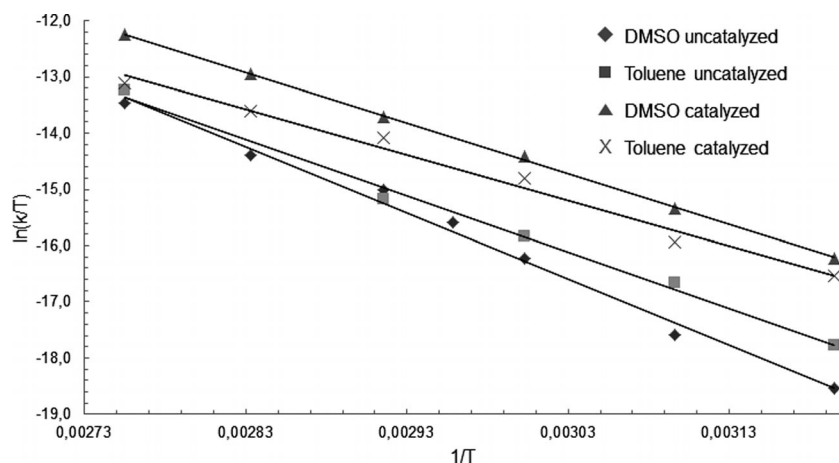
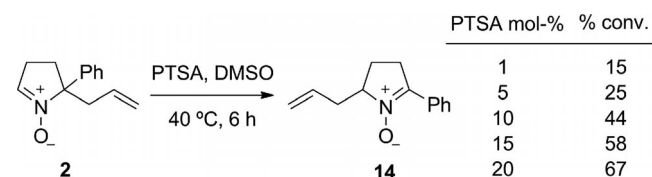


Figure 4. Eyring plots [$\ln(K/T)$ vs. $1/T$] for rearrangement of nitrone **2** in DMSO, toluene, and in the presence of 20 mol-% PTSA.

Table 1. Kinetic parameters for the rearrangements of nitrones 1–3.

Thermodynamic parameters	1	2	3
k (343 K, s^{-1})	1.25×10^{-5}	1.05×10^{-4}	3.87×10^{-5}
E_a (kcal/mol)	22.91	24.06	23.16
ΔH^\ddagger (kcal/mol)	22.23	23.40	21.68
ΔS^\ddagger (cal/K mol)	-16.68	-9.25	-15.17
ΔG^\ddagger (298.15 K, kcal/mol)	27.20	26.15	26.20

in aromatic solvents. Three acid catalysts (CSA, PTSA and phosphoric acid) were tested for the rearrangement of nitrone **2**, with the best results being obtained for CSA and PTSA. In particular, the optimization study carried out for the PTSA-catalyzed process showed that 20 mol-% catalyst was necessary to achieve good conversion (Scheme 6). In the case of acid-catalyzed reactions, nitrone **14** was obtained as the only product of the reaction and no cycloaddition was observed.



Scheme 6. Optimization study for the PTSA-catalyzed rearrangement of nitrone **2e**.

The rearrangement of **2** in toluene exhibited a first-order rate constant k (70 °C) = $8.72 \times 10^{-5} s^{-1}$ from which the activation energy (E_a) was calculated to be 20.61 kcal/mol (Table 2). This value is clearly lower than that found for the rearrangement in DMSO ($E_a = 24.06$ kcal/mol), in agreement with a neutral rearrangement proceeding through a pericyclic transition state. The rate constant for the rearrangement of **2** in DMSO and in the presence of 20 mol-% PTSA was higher [k (70 °C) = $3.83 \times 10^{-4} s^{-1}$] than in the absence of acid [k (70 °C) = $1.05 \times 10^{-5} s^{-1}$]. Accordingly, the activation energy was lower ($E_a = 18.57$ kcal/mol). When the acid-catalyzed process was carried out in toluene

at a rate constant k (70 °C) = $2.61 \times 10^{-4} s^{-1}$ was found. In this case, the activation energy was $E_a = 16.79$ kcal/mol. The Eyring plots for the acid-catalyzed rearrangement of nitrone **2** are illustrated in Figure 4 and the corresponding thermodynamic parameters are given in Table 2.

Table 2. Kinetic parameters for the rearrangements of nitrone **2**.

Thermodynamic parameters	DMSO		Toluene	
	uncatalyzed	catalyzed	uncatalyzed	catalyzed
k (343 K, s^{-1})	1.05×10^{-5}	3.83×10^{-4}	8.72×10^{-5}	2.61×10^{-4}
E_a (kcal/mol)	24.06	18.57	20.61	16.79
ΔH^\ddagger (kcal/mol)	23.40	17.90	19.94	16.12
ΔS^\ddagger (cal/K mol)	-9.25	-21.79	-18.76	-28.52
ΔG^\ddagger (298.15 K, kcal/mol)	26.15	24.40	25.54	24.62

These studies reveal that the rearrangement performed in the presence of 20 mol-% PTSA have lower transition state energies than those of the uncatalyzed reaction. The catalyzed process in toluene is faster than the corresponding process in DMSO but with a minor difference (1.78 kcal/mol) in the values of E_a with respect to the uncatalyzed rearrangements (3.45 kcal/mol). This observation is in agreement with a typical cationic 2-aza-Cope rearrangement for the catalyzed processes in which the stability of the transition structures could be increased, to some extent, in polar solvents such as DMSO.

DFT Calculations

To explore the energetics of the 2-aza-Cope rearrangements studied above, we also performed DFT calculations with both B3LYP^[28] and M06-2X^[29] functionals using the 6-311+G(d,p)^[30] basis set. B3LYP calculations have been reported to provide accurate results in the study of Cope rearrangements,^[31] although in the case of protonated species they lead to an underestimation of the activation energies, indicating insufficient consideration of the electronic correlation effects.^[32] On the other hand, Thrular's func-

FULL PAPER

tionals^[33] have emerged as powerful tools that provide more accurate energy values in several types of reactions.^[34] All the geometry optimizations were carried out with the Gaussian 09 suite of programs.^[35] The solvent effect was computed by using the polarizable continuum model (PCM),^[36] considering both DMSO and toluene as solvents. Calculations for nitrones **1** and **2** were performed with the complete model. In the case of nitrone **3**, the substrate was slightly simplified by replacing the benzyl groups by methyl groups.

The theoretical treatment involved optimization of nitrones **1–3** and **13**, **14** and **17** as well as transition state structures for the interconversion between them. The computed reaction barriers are given in Table 3 and the geometrical structures of the transition states are illustrated in Figure 5.

Table 3. Experimental and calculated activation energies (ΔG^\ddagger , kcal/mol) at 298.15 K for the rearrangement of nitrones **1–3** in DMSO as solvent.

Nitrone	Exp.	Calcd.	
		M06-2X	B3LYP
1	27.20	31.85	30.68
2	26.15	29.46	28.14
3	26.20	27.08	27.15

For *C*-phenyl nitrones **2** and **3** the presence of benzyloxy-methyl substituents does not strongly influence the geometric or energetic features of the transition state. In both cases, the forming C1–C4 bond is longer (1.85–1.86 Å) than the breaking C2–C5 bond (1.75–1.79 Å) and similar N3–C2–C5 and N3–C1–C4 angles are observed (100–101°). On the other hand, **TS1** corresponding to rearrangement of *C*-(methoxycarbonyl) nitrone **1** presents a forming C1–C4 bond (1.70–1.74 Å) shorter than the breaking C2–C5 bond (1.81 Å). Consequently, it appears that **TS2** and **TS3** (corresponding to *C*-phenyl nitrones **2** and **3**, respectively) are earlier transition states than **TS1**. The N3–C2–C5 and N3–C1–C4 angles are similar (101.4° and 102.7°, respectively) to those observed for **TS2** and **TS3**. Indeed, in all cases, the located transition states have a chair-like conformation that is in agreement with a typical Cope rearrangement. The axial disposition of the nitrone oxygen is determined by the required orientation of the orbitals involved in the rearrangement.

Table 3 gives a comparison between experimental and calculated free energies for the rearrangement of nitrones **1–3**. The predictions are not very sensitive to variation in functional and with both B3LYP and M06-2X the predicted energy barrier was higher than that observed experimen-

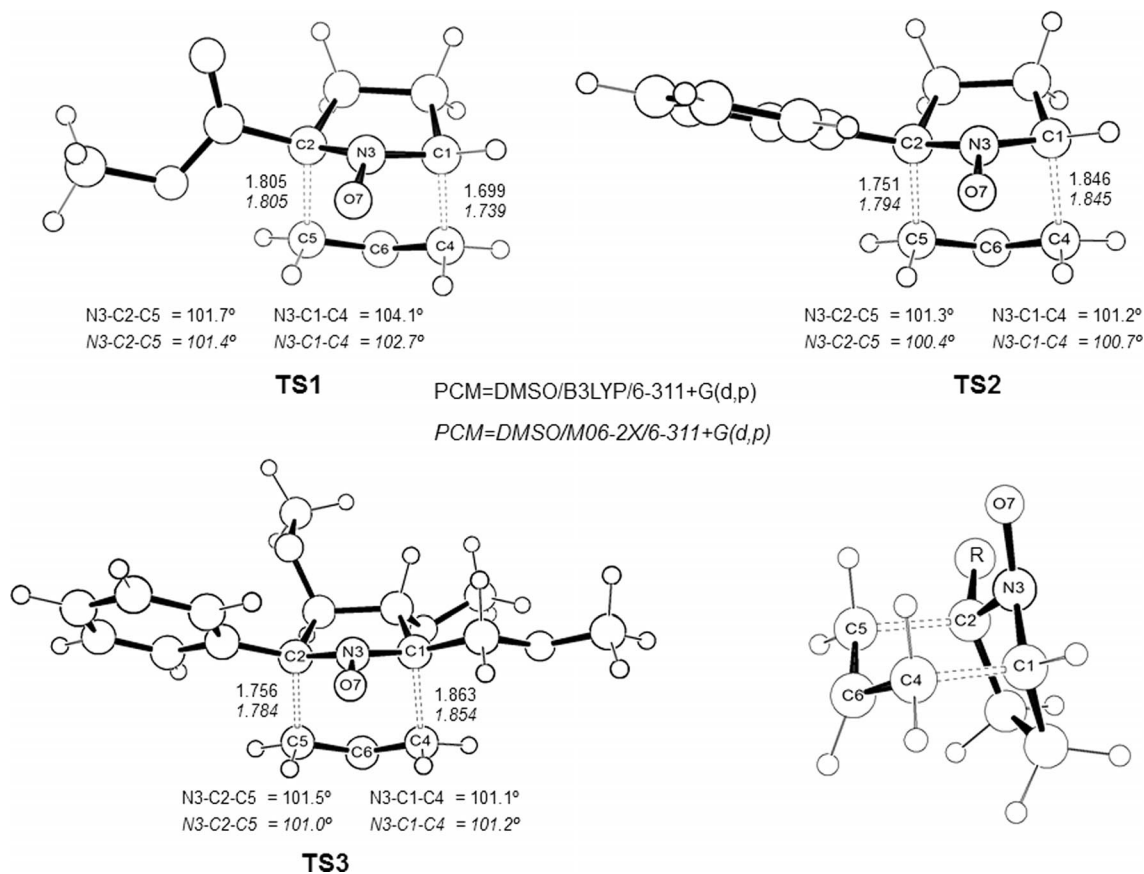


Figure 5. Calculated [PCM(DMSO)/B3LYP/6-311+G(d,p) and PCM(DMSO)/M06-2X/6-311+G(d,p)] transition structures for the rearrangement of nitrones **1–3**. Bond lengths (Å) and activation energies (kcal/mol) at 298.15 K. **TS1** corresponds to the rearrangement of nitrone **1** into **13**; **TS2** corresponds to the rearrangement of nitrone **2** into **14**; **TS3** corresponds to the rearrangement of nitrone **3** into **15**.

tally. Closer values to experimental were observed with B3LYP calculations and, in the case of nitrones **2** (TS2) and **3** (TS3), a difference of less than 2 kcal/mol was obtained. The calculations were not so accurate for nitrone **1** (TS1)

since differences of 3.48 (B3LYP) and 4.65 (M06-2X) kcal/mol were observed. Nevertheless, the calculations reflect the experimentally observed trend that nitrone **1** has a higher activation barrier than those corresponding to nitrones **2**

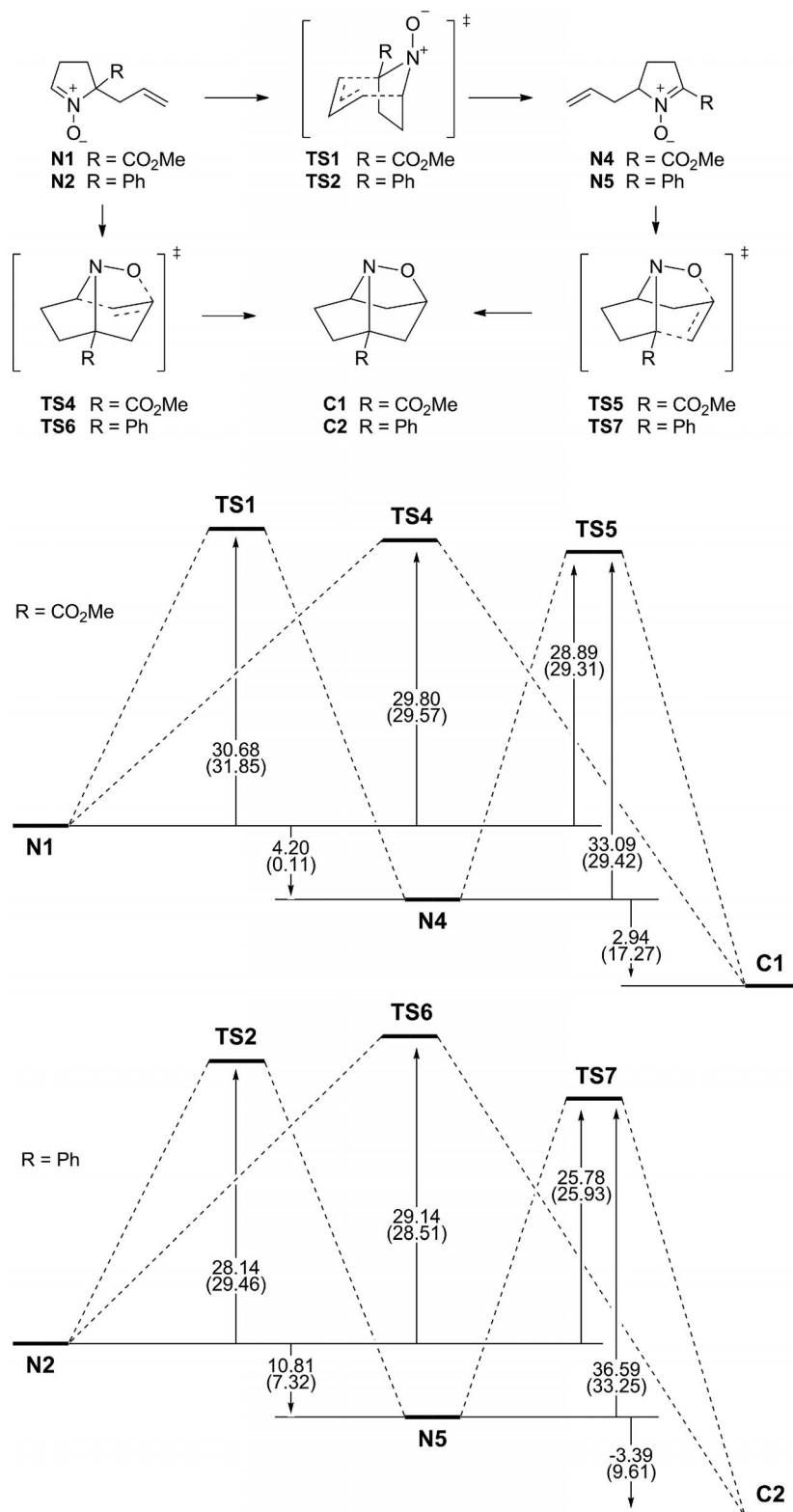


Figure 6. Calculated [PCM(DMSO)/B3LYP/6-311+G(d,p) (plain text) and PCM(DMSO)/M06-2X/6-311+G(d,p) (in parentheses)] energy profiles for the rearrangements of nitrones **1** and **2** into **13** and **14**, respectively, and intramolecular cycloadditions to give cycloadducts **15** and **16**. Relative energies are given in kcal/mol.

FULL PAPER

and **3**, which have similar values (compare Table 3, entry 1 and entries 2–3).

We also located the corresponding transition structures for the intramolecular dipolar cycloaddition leading to cycloadducts **15**, **16** and **18**. In principle, these cycloadducts could be formed from both starting and rearranged nitrones through different transition structures. For nitrone **1** (**N1**), both B3LYP and M06-2X calculations predict the direct intramolecular cycloaddition from nitrone **N1** (through **TS4**) as the most favored process and the 2-aza-Cope rearrangement as less favored (Figure 6). However, the small energy differences between **TS1** and **TS4** (less than 1 kcal/mol in B3LYP calculations) are in agreement with the experimental observations that both processes are observed simultaneously. Indeed, although **TS5** is lower in energy than **TS4** [0.91 kcal/mol (B3LYP) or only 0.21 kcal/mol (M06-2X)], the possibility that the cycloadduct could also be obtained directly from nitrone **1** (**N1**) through **TS4** cannot be discarded.

For nitrone **2** (**N2**), both B3LYP and M06-2X also predict the intramolecular cycloaddition from the rearranged nitrone (through **TS7**) as the most favored process (Figure 6). In this case, however, the 2-aza-Cope rearrangement (through **TS2**) is predicted to be more favored than the direct cycloaddition from **N2** (through **TS6**) by 1.0 kcal/mol

(B3LYP). The predicted energy differences between **TS2** and **TS7** (and **TS6**) agree with the experimentally observed higher ratio between nitrone **14** and cycloadduct **16** (6:1) with respect to that observed between nitrone **13** and cycloadduct **15** (3:2) (Scheme 5).

In the case of nitrone **3**, similar results were observed with both B3LYP and M06-2X functionals. The calculated energy differences are similar to those observed for nitrone **2** (**N2**) (see the Supporting Information).

DFT calculations on 2-aza-Cope rearrangements of nitrone **2** considering toluene as a solvent and under catalytic conditions were also performed. The geometrical structures of the transition states are depicted in Figure 6 and the corresponding free energy barriers are given in Table 4.

Table 4. Experimental and calculated activation energies (ΔG^\ddagger , kcal/mol) at 298.15 K for the rearrangement of nitrone **2**.

Solvent	Catalyzed	Exp.	Caled. M06-2X	B3LYP
DMSO	no	26.15	29.46	28.14
Toluene	no	25.54	27.39	28.08
DMSO	yes	24.40	19.43	20.98
Toluene	yes	24.62	19.00	20.26

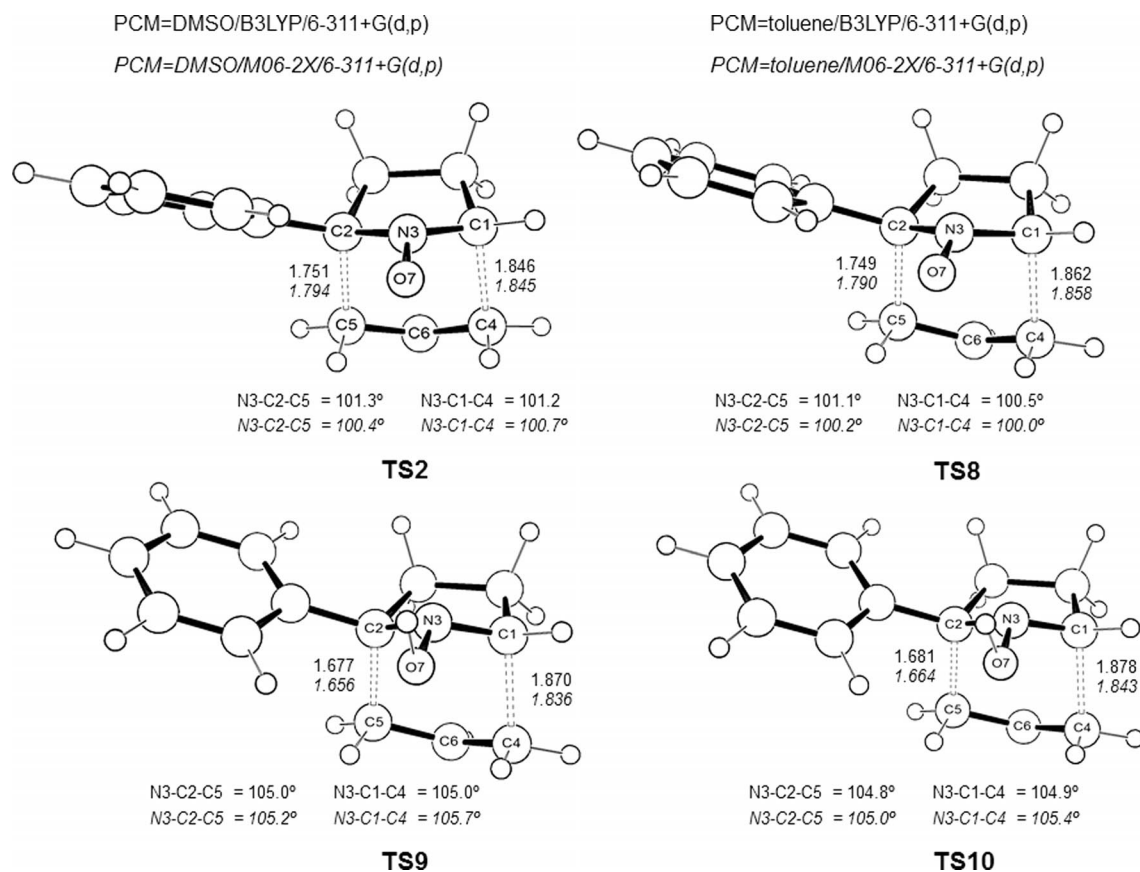


Figure 7. Calculated [PCM(DMSO)/B3LYP/6-311+G(d,p) and PCM(DMSO)/M06-2X/6-311+G(d,p)] transition structures for the rearrangement of nitrone **2** into **14**. Bond lengths (Å) and activation energies (kcal/mol) at 298.15 K. **TS2** and **TS8** correspond to the rearrangement in DMSO and toluene, respectively; **TS9** and **TS10** correspond to the PTSA-catalyzed rearrangement in DMSO and toluene, respectively.

For the uncatalyzed reaction, both B3LYP and M06-2X calculations reflect the observed slight acceleration of the reaction when solvent was changed from DMSO to toluene. Again, B3LYP calculations proved to be more accurate, predicting a negligible difference (0.06 kcal/mol), in agreement with that observed experimentally (0.61 kcal/mol). The observed overestimation of calculated energy barriers of 2–3 kcal/mol for DMSO was reproduced for toluene. The geometry of the transition states in DMSO (**TS2**) and toluene (**TS8**) are quite similar, with very close values of forming C1–C4 bonds (1.85 Å in DMSO and 1.86 Å in toluene) and breaking C2–C5 bonds (1.75 Å in both DMSO and toluene). Similarly, no remarkable variations were observed in N3–C2–C5 and N3–C1–C4 angles (see Figure 7).

In the case of catalyzed rearrangement of nitrene **2**, we considered protonated species at the nitrene oxygen (Figure 7). Calculations reflect the observed acceleration of the process, predicting lower energy barriers in all cases. In contrast to calculations corresponding to the neutral process,

the energy barriers for the cationic rearrangement are underestimated in both B3LYP and M06-2X calculations, and lower barriers than those observed experimentally are predicted (Table 4).

As expected for a cationic rearrangement, transition states **TS9** and **TS10** are more asynchronous than their respective counterparts **TS2** and **TS8**. Consequently, whereas the breaking C2–C5 bond is shortened (from 1.75 to 1.68 Å in DMSO and toluene), the forming C1–C4 bond is slightly lengthened (from 1.85 to 1.87 Å in DMSO and from 1.86 to 1.88 Å in toluene).

When the cycloaddition process was considered, the calculations were found to reflect the observed experimental results. For protonated species, the intramolecular cycloaddition is disfavored both kinetically (high energy barriers for **TS11** and **TS12**) and thermodynamically (the protonated cycloadduct is less stable than the corresponding protonated nitrenes). In consequence, the calculations correctly predict that only the rearranged nitrene would be obtained (Figure 8).

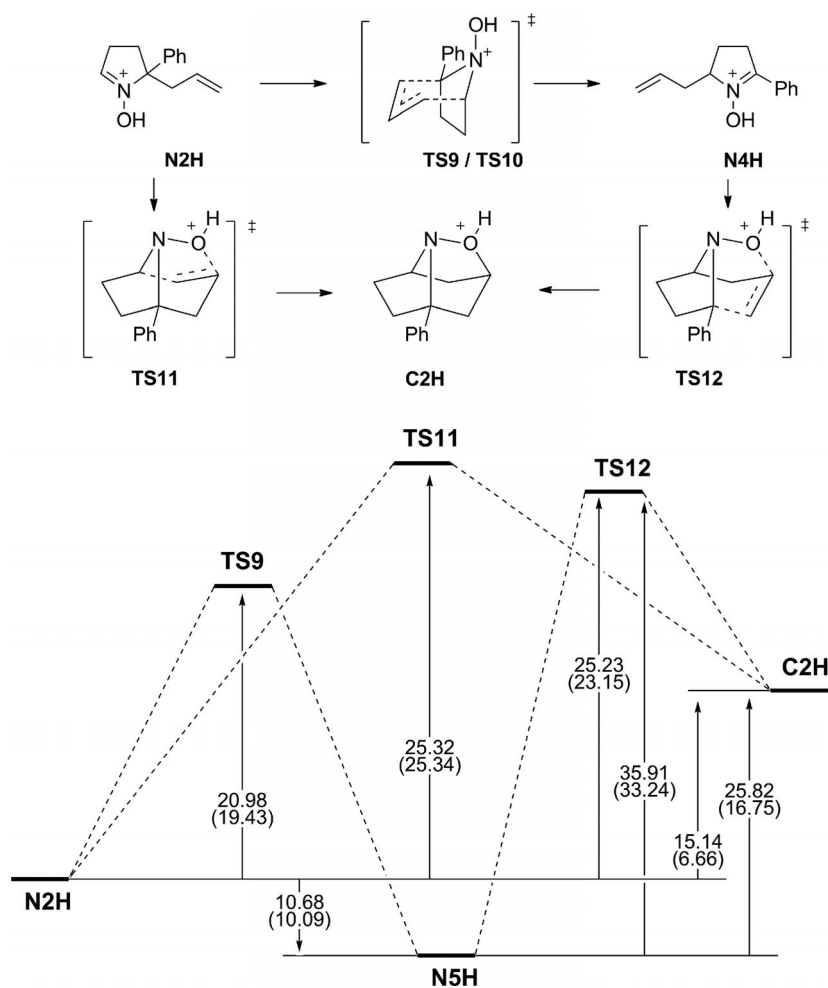


Figure 8. Calculated [PCM(DMSO)/B3LYP/6-311+G(d,p) (plain text) and PCM(DMSO)/M06-2X/6-311+G(d,p) (in parentheses)] energy profiles for the PTSA-catalyzed rearrangement of nitrene **2** into **14** and intramolecular cycloaddition to give protonated cycloadduct **16**. Relative energies are given in kcal/mol. **TS9** and **TS10** correspond to the rearrangement in DMSO and toluene, respectively.

FULL PAPER

Conclusions

We have studied the first reported neutral 2-aza-Cope rearrangement of nitrones both experimentally (kinetically) and theoretically to determine the main factors affecting the process. Kinetic studies reveal that the rearrangement is favored in aromatic solvents, in agreement with an aromatic transition state. Acid catalysis accelerates the process and diminishes the difference between aromatic and polar solvents. These results clearly demonstrate that whereas the uncatalyzed process occurs through a neutral transition state, the catalyzed process takes place through cationic species. In spite of these observations, the aromaticity of the transition state favors in all cases the reaction conducted in an aromatic solvent (toluene). DFT calculations support these results and predict an activation energy barrier for the rearrangement that is in reasonable agreement with the kinetic experimental observations. The observed ratios between rearranged nitrones and cycloadducts are supported in part by calculations. Small energy differences are obtained with both B3LYP and M06-2X calculations (in most cases within experimental error) and, in consequence, it is not possible to describe accurately the process despite that high level calculations [6-311+G(d,p) basis set] have been carried out. The complete stereoselectivity observed for nitrone **3** is well-supported by DFT calculations since a pericyclic process with complete transfer of chirality is predicted for the rearrangement.

Experimental Section

General Procedure for the Rearrangement of Nitrones 1–3: A solution of the corresponding nitrone (1 mmol) was dissolved in anhydrous DMSO (25 mL), placed in a sealed tube and heated at 70 °C under an argon atmosphere for 6 h, at which time the solvent was partially evaporated and the resulting solution was filtered through a pad of silica gel. After washing the silica with diethyl ether, the resulting solution was evaporated under reduced pressure and the residue was purified by column chromatography (hexane/EtOAc, 4:1).

2-Allyl-5-(methoxycarbonyl)-3,4-dihydro-2H-pyrrole 1-Oxide (13): ¹H NMR (300 MHz, CDCl₃): δ = 1.90–1.96 (m, 1 H), 2.42–2.52 (m, 1 H), 2.74–2.79 (m, 1 H), 2.80–2.86 (m, 2 H), 3.80 (s, 3 H), 4.15–4.20 (m, 1 H), 5.11–5.17 (m, 2 H), 5.64 (ddt, *J* = 7.1, 10.2, 17.2 Hz, 1 H) ppm. ¹³C NMR (75 MHz, CDCl₃): δ = 25.5, 31.0, 41.5, 45.8, 52.7, 64.1, 79.2, 160.2, 174.1 ppm.

2-Allyl-5-phenyl-3,4-dihydro-2H-pyrrole 1-Oxide (14): ¹H NMR (300 MHz, CDCl₃): δ = 1.90 (ddd, *J* = 6.8, 9.1, 13.3 Hz, 1 H), 2.25 (ddd, *J* = 7.0, 8.1, 13.3 Hz, 1 H), 2.50–2.57 (m, 1 H), 2.77–2.84 (m, 1 H), 2.98–3.04 (m, 2 H), 4.18–4.26 (m, 1 H), 5.05–5.15 (m, 2 H), 5.7 (ddt, *J* = 7.1, 10.2, 17.2 Hz, 1 H), 7.32–7.40 (m, 3 H), 8.25–8.31 (m, 2 H) ppm. ¹³C NMR (75 MHz, CDCl₃): δ = 27.1, 39.7, 48.1, 64.1, 119.9, 125.5, 126.7, 128.4, 133.6, 134.6, 135.3 ppm. C₁₃H₁₅NO (201.27): calcd. C 77.58, H 7.51, N 6.96; found C 77.64, H 7.41, N 7.06.

(2R,3R,4R)-2-Allyl-3,4-bis(benzyloxy)-2-[(benzyloxy)methyl]-5-phenyl-3,4-dihydro-2H-pyrrole 1-Oxide (15): [*a*]_D²⁵ = +8 (*c* = 0.35, CHCl₃). ¹H NMR (500 MHz, CDCl₃): δ = 2.54 (d, *J* = 7.1 Hz, 2 H), 3.53 (d, *J* = 10.2 Hz, 1 H), 4.22 (d, *J* = 10.2 Hz, 1 H), 4.33 (d,

J = 11.5 Hz, 1 H), 4.50 (d, *J* = 11.7 Hz, 1 H), 4.51 (d, *J* = 11.5 Hz, 1 H), 4.67 (d, *J* = 11.2 Hz, 1 H), 4.69 (d, *J* = 11.5 Hz, 1 H), 4.74 (d, *J* = 11.8 Hz, 1 H), 4.80 (d, *J* = 4.3 Hz, 1 H), 5.01 (dd, *J* = 10.2, 2.0 Hz, 1 H), 5.15 (ddt, *J* = 17.1, 2.1, 1.2 Hz, 1 H), 5.33 (d, *J* = 4.3 Hz, 1 H), 5.82 (ddt, *J* = 17.4, 10.1, 7.3 Hz, 1 H), 7.10–7.13 (m, 2 H), 7.26–7.32 (m, 8 H), 7.34–7.41 (m, 5 H), 7.43–7.47 (m, 3 H), 8.41–8.45 (m, 2 H) ppm. ¹³C NMR (125 MHz, CDCl₃): δ = 34.9, 68.5, 71.2, 72.8, 73.6, 78.5, 82.1, 83.7, 120.1, 127.7, 127.8, 127.8, 127.8, 128.0, 128.2, 128.3, 128.4, 128.5, 130.2, 131.7, 137.6, 137.7, 137.8, 139.1 ppm. C₃₅H₃₅NO₄ (533.67): calcd. C 78.77, H 6.61, N 2.62; found C 78.54, H 6.40, N 2.45.

General Procedure for the Catalyzed Rearrangement of Nitrone 2: A solution of nitrone **2** (0.201 g, 1 mmol) was dissolved in anhydrous DMSO (25 mL), treated with *p*-toluenesulfonic acid (34 mg, 0.2 mmol), placed in a sealed tube, and heated at 40 °C under an argon atmosphere for 6 h, at which time the solvent was partially evaporated and the resulting solution was filtered through a pad of silica gel. After washing the silica with diethyl ether, the resulting solution was evaporated under reduced pressure and the residue was purified by column chromatography (hexane/EtOAc, 4:1).

Supporting Information (see footnote on the first page of this article): Experimental procedures for the preparation of nitrones **1–3**. Arrhenius plots of kinetically studied reactions. Experimental details of NMR kinetic experiments. Additional computational details including energy diagrams, tables with absolute and relative electronic and free energies, and coordinates of stationary points (nitrones, transition structures and cycloadducts). Copies of ¹H and ¹³C NMR spectra.

Acknowledgments

The authors thank for support by the Spanish Ministry of Science and Innovation (MICINN) (project number CTQ2010-19606), by the European Union (EU) (FEDER Program) and by the Government of Aragon (Research group E-10, Zaragoza, Spain). A. M. thanks the European Commission and European Social Fund (POR Calabria 2007/2013) for a grant.

- [1] a) J. Zeh, M. Hiersemann, in: *Stereoselective Synthesis 3. Stereoselective pericyclic reactions, cross-coupling and C–H and C–X Activation*, vol. 3 (Ed.: P. A. Evans). Thieme, Stuttgart, Germany, New York **2011**, p. 347–382; b) E. A. Iardi, C. E. Stivala, A. Zkarian, *Chem. Soc. Rev.* **2009**, *38*, 3133–3148; c) U. Nubbemeyer, *Synthesis* **2003**, 961–1008.
- [2] a) *The Claisen rearrangement: Methods and Applications* (Eds.: M. Hierseman, U. Nubbemeyer), Wiley-VCH, Weinheim, Germany, **2007**; b) H. Ito, T. Taguchi, *Chem. Soc. Rev.* **1999**, *28*, 43–50; c) A. M. M. Castro, *Chem. Rev.* **2004**, *104*, 2939–3002.
- [3] a) J. J. Rhoad, N. R. Raulins, *Org. React.* **1975**, *22*, 1–252; b) R. K. Hill, in: *Comprehensive Organic Synthesis* (Eds.: B. M. Trost, I. Fleming), Pergamon Press, Oxford, UK, vol. 5, p. 785–826; c) L. A. Paquette, *Tetrahedron* **1997**, *53*, 13971–14020.
- [4] M. P. McCormack, T. Shalumova, J. M. Tanski, S. P. Waters, *Org. Lett.* **2010**, *12*, 3906–3909.
- [5] a) J. Royer, M. Bonin, L. Micouin, *Chem. Rev.* **2004**, *104*, 2311–2352; b) L. Overman, *Acc. Chem. Res.* **1992**, *25*, 352–359.
- [6] M. Chu, P. L. Wu, S. Giure, F. W. Fowler, *Tetrahedron Lett.* **1986**, *27*, 461–464.
- [7] a) P.-L. Wu, F. W. Fowler, *J. Org. Chem.* **1988**, *53*, 963–972; b) P.-L. Wu, F. W. Fowler, *J. Org. Chem.* **1988**, *53*, 5998–6005.
- [8] a) G. R. Cook, N. S. Barta, J. R. Stille, *J. Org. Chem.* **1992**, *57*, 461–467; b) L. G. Beholz, J. R. Stille, *J. Org. Chem.* **1993**, *58*, 5095–5100.
- [9] D. F. McComsey, B. E. Maryanoff, *J. Org. Chem.* **2000**, *65*, 4938–4943.

- [10] T. A. Geissman, R. M. Horowitz, *J. Am. Chem. Soc.* **1950**, *72*, 1518–1522.
- [11] a) M. Geisel, C. A. Grob, R. A. Wohl, *Helv. Chim. Acta* **1969**, *52*, 2206–2215; b) J. A. Marshall, J. H. Babler, *J. Org. Chem.* **1969**, *34*, 4186–4188; c) C. A. Grob, N. Kunz, P. R. Marbet, *Tetrahedron Lett.* **1975**, *16*, 2613–2616.
- [12] Y. Gelas-Mialhe, J.-C. Gramain, A. Louvet, R. Remuson, *Tetrahedron Lett.* **1992**, *33*, 73–76.
- [13] K. M. Brummond, J. Lu, *Org. Lett.* **2001**, *3*, 1347–1349.
- [14] a) A. Madin, C. J. O'Donnell, T. Oh, D. W. Old, L. E. Overman, *Angew. Chem.* **1999**, *111*, 3110; *Angew. Chem. Int. Ed.* **1999**, *38*, 2934–2936; b) M. Sugiura, C. Mori, S. Kobayashi, *J. Am. Chem. Soc.* **2006**, *128*, 11038–11039; c) Z. D. Aron, L. E. Overman, *Org. Lett.* **2005**, *7*, 913–916; d) K. M. Brummond, S.-P. Hong, *J. Org. Chem.* **2005**, *70*, 907–916; e) L. A. Overman, M. Kakimoto, *J. Am. Chem. Soc.* **1979**, *101*, 1310–1312; f) S. D. Knight, L. A. Overman, G. Pairedeau, *J. Am. Chem. Soc.* **1993**, *115*, 9293–9294; see also ref. 11–13.
- [15] M. Rueping, A. P. Antonchick, *Angew. Chem. Int. Ed.* **2008**, *47*, 1090–1093.
- [16] P. G. M. Wuts, Y.-W. Jung, *J. Org. Chem.* **1988**, *53*, 1957–1965.
- [17] H.-S. Cheng, A.-W. Seow, T.-P. Loh, *Org. Lett.* **2008**, *10*, 2805–2807.
- [18] R. W. Hoffmann, A. Endesfelder, *Liebigs Ann. Chem.* **1986**, 1823–1836.
- [19] P. Merino, T. Tejero, V. Mannucci, *Tetrahedron Lett.* **2007**, *48*, 3385–3388.
- [20] For two recent cases in which we observed experimental evidence for such rearrangements, see: a) I. Delso, T. Tejero, A. Goti, P. Merino, *J. Org. Chem.* **2011**, *76*, 4139–4143; b) E. Marca, I. Delso, T. Tejero, P. Merino, *Tetrahedron* **2012**, *68*, 6674–6687.
- [21] A. Goti, L. Nanelli, *Tetrahedron Lett.* **1996**, *37*, 6025–6028.
- [22] R. W. Murray, K. Iyanar, J. Chen, J. T. Wearing, *J. Org. Chem.* **1996**, *61*, 8099–8102.
- [23] S.-I. Murahashi, H. Mitsui, T. Shiota, T. Tsuda, S. Watanabe, *J. Org. Chem.* **1990**, *55*, 1736–1744.
- [24] P. Merino, I. Delso, V. Mannucci, T. Tejero, *Tetrahedron Lett.* **2006**, *47*, 3311–3314.
- [25] a) S. Cicchi, M. Marradi, A. Goti, A. Brandi, *Tetrahedron Lett.* **2001**, *42*, 6503–6505; b) A. Goti, S. Cicchi, V. Mannucci, F. Cardona, F. Guarna, P. Merino, T. Tejero, *Org. Lett.* **2003**, *5*, 4235–4238.
- [26] O. N. Burchak, C. Philouze, P. Y. Chavant, S. Py, *Org. Lett.* **2008**, *10*, 3021–3023.
- [27] a) P. Merino, I. Delso, T. Tejero, F. Cardona, A. Goti, *Synlett* **2007**, 2651–2654; b) F. Cardona, E. Faggi, M. Liguori, A. Cacciarini, A. Goti, *Tetrahedron Lett.* **2003**, *44*, 2315–2318.
- [28] B3LYP is a combination of Becke's three-parameter hybrid exchange functional B3 (A. D. Becke, *J. Am. Phys.* **1993**, *98*, 5648–5652) with the electronic correlation functions of Lee, Yang and Parr (C. Lee, W. Yang, R. G. Parr, *Phys. Rev. B* **1988**, *37*, 785–789).
- [29] a) Y. Zhao, D. G. Thrular, *Theor. Chem. Acc.* **2008**, *10*, 215–241; b) Y. Zhao, D. G. Thrular, *J. Phys. Chem. A* **2006**, *110*, 13126–13130; c) Y. Zhao, D. G. Thrular, *J. Chem. Phys.* **2006**, *125*, 194101–194119.
- [30] K. Raghavachari, J. S. Binkley, R. Seeger, J. A. Pople, *J. Chem. Phys.* **1980**, *72*, 650–654.
- [31] a) D. A. Hrovat, J. Chen, K. N. Houk, W. T. Borden, *J. Am. Chem. Soc.* **2000**, *122*, 7456–7460; b) I. Ozkan, M. Zora, *J. Org. Chem.* **2003**, *68*, 9635–9642; c) C. F. Weise, S. Immer, F. Richter, C. Schneider, *Eur. J. Org. Chem.* **2012**, 1520–1529; d) D. J. Babinski, X. Bad, M. E. Arba, B. Chen, D. A. Hrovat, W. T. Borden, D. E. Frantz, *J. Am. Chem. Soc.* **2012**, *134*, 16139–16142.
- [32] R. F. Winter, G. Rauhut, *Chem. Eur. J.* **2002**, *8*, 641–649.
- [33] Y. Zhao, D. G. Thrular, *Acc. Chem. Res.* **2008**, *41*, 157–167.
- [34] a) S. E. Wheeler, A. Moran, S. N. Pieniazek, K. N. Houk, *J. Phys. Chem. A* **2009**, *113*, 10376–10384; b) Y. Zhao, D. G. Thrular, *J. Chem. Theory Comput.* **2009**, *5*, 324–333; c) X. Xuefei, I. M. Alecu, D. G. Thrular, *J. Chem. Theory Comput.* **2011**, *7*, 1667–1676; d) S. Steinman, M. D. Wodrich, C. Corminboeuf, *Theor. Chem. Acc.* **2010**, *127*, 492–442.
- [35] M. J. Frisch, G. W. Trucks, H. B. Schlegel, G. E. Scuseria, M. A. Robb, J. R. Cheeseman, G. Scalmani, V. Barone, B. Mennucci, G. A. Petersson, H. Nakatsuji, M. Caricato, X. Li, H. P. Hratchian, A. F. Izmaylov, J. Bloino, G. Zheng, J. L. Sonnenberg, M. Hada, M. Ehara, K. Toyota, R. Fukuda, J. Hasegawa, M. Ishida, T. Nakajima, Y. Honda, O. Kitao, H. Nakai, T. Vreven, J. A. Montgomery Jr., J. E. Peralta, F. Ogliaro, M. Bearpark, J. J. Heyd, E. Brothers, K. N. Kudin, V. N. Staroverov, R. Kobayashi, J. Normand, K. Raghavachari, A. Rendell, J. C. Burant, S. S. Iyengar, J. Tomasi, M. Cossi, N. Rega, J. M. Millam, M. Klene, J. E. Knox, J. B. Cross, V. Bakken, C. Adamo, J. Jaramillo, R. Gomperts, R. E. Stratmann, O. Yazyev, A. J. Austin, R. Cammi, C. Pomelli, J. W. Ochterski, R. L. Martin, K. Morokuma, V. G. Zakrzewski, G. A. Voth, P. Salvador, J. J. Dannenberg, S. Dapprich, A. D. Daniels, Ö. Farkas, J. B. Foresman, J. V. Ortiz, J. Cioslowski, D. J. Fox, *Gaussian 09*, revision A.1, Gaussian, Inc., Wallingford CT, **2009**.
- [36] a) J. Tomasi, B. Mennucci, R. Cammi, *Chem. Rev.* **2005**, *105*, 2999–3094; b) B. Mennucci, J. Tomasi, R. Cammi, J. R. Cheeseman, M. J. Frisch, F. J. Devlin, S. Gabriel, P. J. Stephens, *J. Phys. Chem. A* **2002**, *106*, 6102–6113.

Received: June 6, 2013

Published Online: ■